Osaka, Japan), as described previously.[24] Briefly, 2×10^5 R28 cells were cultured in 24-well plates (500 μl medium per well) with or without hydrogen peroxide (1 mM; Merck, Darmstadt, Germany) for 24 h. Then the cells were incubated with MTT (0.5 mg/ml; final concentration) for 3 h. Formazan product was solubilized by the addition of dimethyl sulfoxide for 16 h. Dehydrogenase activity was expressed as absorbance at a test wavelength of 570 nm and at a reference wavelength of 630 nm. Assays were performed in triplicate and repeated three times in independent experiments.

Immunofluorescence for HMGB1 and TUNEL

Indirect immunofluorescence was carried out as described previously,[19,25] with some modifications. The eyes were harvested and fixed in 4% paraformaldehyde at 4°C overnight. The anterior segment and the lens were removed, and the remaining eye cup was cryoprotected with 10–30% sucrose in phosphate-buffered saline. The eye cups were then frozen in an optimal cutting temperature compound (Sakura Finetech, Tokyo, Japan). Sections were cut at 8 μm with a cryostat (Leica Microsystems, Wetzler, Germany). After being incubated with blocking buffer containing 10% goat serum, 1% bovine serum albumin (BSA), and 0.05% Tween-20 for 1 h, the slides were incubated with rabbit polyclonal anti-HMGB1 antibody (1 μg/ml). After overnight incubation, sections were washed and probed with Alexa-Fluor 594-conjugated goat anti-rabbit IgG F(ab')2 fragment (Molecular Probes, Carlsbad, CA) for 1 h. In some experiments, TUNEL co-staining was also performed according to the manufacturer's protocol (ApopTag Fluorescein *In situ* Apoptosis Detection kit; Chemicon, Temecula, CA) as previously described.[22] Slides were counterstained with DAPI, mounted with Shandon PermaFlour (Thermo Scientific, Waltham, MA), and viewed with a Zeiss fluorescence microscope. Images were captured using the same exposure time for each comparative section. To examine the specificity of immunostaining, the primary antibody was replaced with normal rabbit IgG (1 μg/ml). Control slides were invariably negative under the same setting (data not shown). For all experiments, at least three sections from each eye were evaluated. To demonstrate the expression patterns of HMGB1 in retinal cells under oxidative stress *in vitro*, R28 cells (2×10^5 cells/500 μl medium per well) were seeded on four-well glass coverslips and challenged with or without hydrogen peroxide (1 mM) for 1 h. Slides were fixed in 4% paraformaldehyde for 1 h, permeabilized with Triton X-100, and then examined by the same methods as described above.

ELISAs

HMGB1 and MCP-1 were quantified in each human vitreous sample using commercial ELISAs; HMGB1 ELISA kit (Shino-Test Corporation) and Human CCL2/MCP-1 Immunoassay (R&D Systems, Minneapolis, MN), according to the manufacturers' protocols. The detection limits of these kits were 0.2 ng/ml for HMGB1 and 5.0 pg/ml for MCP-1. Concentrations below the limits were taken as zero in subsequent analyses. Each sample was run in duplicate and compared with a standard curve. All samples were assessed in a masked manner. The mean concentration was determined per sample. For *in vitro* study, HMGB1 levels in culture supernatants were measured by the same ELISA.

Migration Assay

Cell migration was assayed using a modified Boyden chamber assay as previously described.[26] In brief, 5×10^4 ARPE-19 cells resuspended in 200 μl control medium (1% FBS-DMEM/F12) were seeded onto the upper compartment of the BD Falcon® culture inserts (BD Bioscience, San Jose, CA) with an 8-μm diameter pore size membrane in a 24-well companion plate. The lower chamber was filled with control medium (negative control) and those containing 50, 100, or 200 ng/ml rHMGB1. Because MCP-1 was reported to display a potent chemotactic activity on RPE cells,[27] a control medium containing 10 ng/ml rMCP-1 was used as a positive control. After 8-h incubation, cells remaining on the upper surface of the filters were removed mechanically, and those that had migrated to the lower surface were fixed with methanol, stained with Diff-Quick (Dade-Behring, Deerfield, IL), and counted in five randomly selected high-power fields ($\times$ 100) per insert. Migration index (% of control) was calculated by dividing the number of migrating cells in the presence of chemoattractants by the cells that migrated in response to the negative control. To inhibit ERK-1/2 activity, the cells were pretreated with 1, 5, or 10 μM U0126, or vehicle (0.1% dimethyl sulfoxide) for 30 min, prior to the addition of rHMGB1. U0126 is an inhibitor of active and inactive MEK-1/2, the MAPK kinase that activates ERK-1/2. These concentrations of U0126 and dimethyl sulfoxide had no effect on ARPE-19 cell viability determined by MTT assay in our study (data not shown) and in a previous report.[28] Assays were performed in triplicate and repeated three times in independent experiments.

Immunoblotting

ARPE-19 cells (5×10^5) were subcultured on 6-cm tissue culture dishes. Then, the cells were serum starved overnight in DMEM/F12 and stimulated with 100 ng/ml rHMGB1 for the indicated times. Activation of ERK-1/2 was analyzed as described previously.[24] In brief, after treatment, whole cells were lysed with SDS sample buffer and an equal volume of protein extracts was loaded onto 12% SDS-polyacrylamide gels and then transferred onto a nitrocellulose membrane. The membrane was blocked by incubation with 5% non-fat dry milk plus 1% BSA in TBST (0.02% Tween-20 in Tris-buffered saline, pH 7.4) for 1 h at room temperature. The membrane was then incubated with the antibody against phospho-ERK-1/2 (diluted 1/1000) at 4°C overnight. The blots were subsequently probed with secondary anti-rabbit antibodies conjugated to horseradish peroxidase (diluted 1/3000 in TBST), and images were developed using the en-

hanced chemiluminescence system (GE Healthcare). The membrane was stripped and reprobed with an antibody against total ERK-1/2 (diluted 1/1000).

Statistical Analysis

The vitreous HMGB1 and MCP-1 concentrations in each group were compared using the Mann–Whitney *U*-test. The correlation between HMGB1 and MCP-1 in RD samples was analyzed using a simple linear regression analysis and Spearman's rank correlation coefficient. All *in vitro* data are presented as mean ± s.d. and the significance of differences between groups was determined by Student's *t*-test. *P*-value less than 0.05 was considered significant.

RESULTS

HMGB1 is Present in Cultured Retinal Cell and Released Extracellularly by Oxidative Stress-Induced Cell Death

We first evaluated the expression patterns and cellular distribution of HMGB1 in an R28 retinal cell line with or without oxidative stress, a known cause of neurodegeneration.[29] Excessive reactive oxygen species can lead to the destruction of cellular components and ultimately induce cell death through apoptosis or necrosis. To induce oxidative stress, we used a toxic dose (1 mM) of hydrogen peroxide, which was reported to stimulate monocytes/macrophages to release HMGB1 actively and passively.[30] As shown in Figure 1a, HMGB1 immunoreactivity was stably present in the nucleus of unstimulated R28 cells, and relatively weak staining was observed in the cytoplasm. By contrast, 1 h after exposure to 1 mM hydrogen peroxide, some cells seemed to present rather high levels of HMGB1 in their nucleus as well as their cytoplasm compared with those under an unstimulated condition. However, in the other cells, the nuclear HMGB1 was diminished or appeared to be released into the cytoplasm. These results indicate that the nuclear HMGB1 could be varied by death stress and be released into the cytoplasm according to the degree of stress. Hydrogen peroxide (1 mM) treatment for 24 h, in which about 90% of the cells lost their viability (Figure 1b), induced a massive release of HMGB1 from the cells to the cell supernatants (Figure 1c). Taken together, these findings suggested that HMGB1 could relocate from the nucleus to the cytoplasm for eventual release in dying retinal cells, and that the extracellular release of HMGB1 in the eye might be increased dependent on the extent of retinal cell death.

HMGB1 is Abundantly Expressed in Rat Retina and Released after RD

As the above findings indicated that HMGB1 was of relevance to retinal cell death, we investigated whether HMGB1 was maintained in the rat retina and how HMGB1 would vary after RD. As it was reported that HMGB1 in rat photoreceptors had a light-sensitive circadian rhythmic expression,[25] we performed all animal studies on a regular time schedule, and all eyes were set to be almost equally exposed to light. As shown in Figure 2, HMGB1 immunoreactivity was well represented in sections of the normal control rat retina and, as expected, colocalized with DAPI-positive nuclei (Figure 2a, d and g). HMGB1 staining in the normal rat retina was prominent in the nuclei of ganglion cell layer, inner nuclear layer, outer nuclear layer, and RPE, and was also apparent in the photoreceptor inner segments. In particular, HMGB1 was localized in photoreceptor at the nuclear periphery, and HMGB1 levels were higher in the inner nuclear layer than the outer nuclear layer as opposed to DAPI staining, which preferred to bind to heterochromatic DNA. This was consistent with the previous report[25] that HMGB1 was preferentially colocalized with euchromatin, which was often under active transcription and was stained less by DAPI. Interestingly, HMGB1 appeared to be robustly upregulated in both the photoreceptors and the other retinal cells at day 3 after RD inductions, and DAPI staining was inversely downregulated at the same time (Figure 2b, e and h). As previous reports demonstrated that dramatic alterations of retinal gene expression occurred after RD,[31] this high level of HMGB1 expression might be related to the active gene transcription. HMGB1 in the nucleus might be stress responsive and necessary for proper transcription after RD tissue damage. Afterwards, the nuclear HMGB1 expression in the photoreceptors seemed to subside at day 7, while still clearly remained in the inner segments (Figure 2c, f and i), gradually decreasing along with the thinning of the outer nuclear layer due to photoreceptor degeneration by day 14 (data not shown).

Although HMGB1 expression was increased in the photoreceptors of the detached retina at day 3, it was not homogeneous, but was rather heterogeneous. To clarify the relationship between the upregulation of HMGB1 and photoreceptor cell death, especially with DNA damage, the RD retina at day 3 was co-stained with TUNEL, which could detect apoptotic and potentially necrotic cell death by labeling the damaged DNA (Figure 3a–c). Previous studies indicated that HMGB1 could not be released from apoptotic cells[6] and the apoptotic photoreceptors were prominent in this RD model at day 3 after RD.[22] We also confirmed remarkable numbers of apoptotic photoreceptors in the detached retina at day 3 (Figure 3b), and found that the early faint TUNEL-positive nuclei had relatively low levels of HMGB1 and fragmented nuclei, which were brightly stained by TUNEL, had almost no apparent HMGB1 immunoreactivity (Figure 3c), suggesting that apoptotic dying cells might lose the expression of HMGB1 to maintain the proper gene transcription. It might be indispensable for the surviving photoreceptors to maintain and/or boost the nuclear HMGB1 in RD.

In the subretinal space of RD at day 7, HMGB1-positive and TUNEL-negative debris could be observed (Figure 3d, arrows), which might be released by necrotic photoreceptors and/or degradated inner segments, and spread diffusely into the vitreous cavity if a retinal break was present. It was also

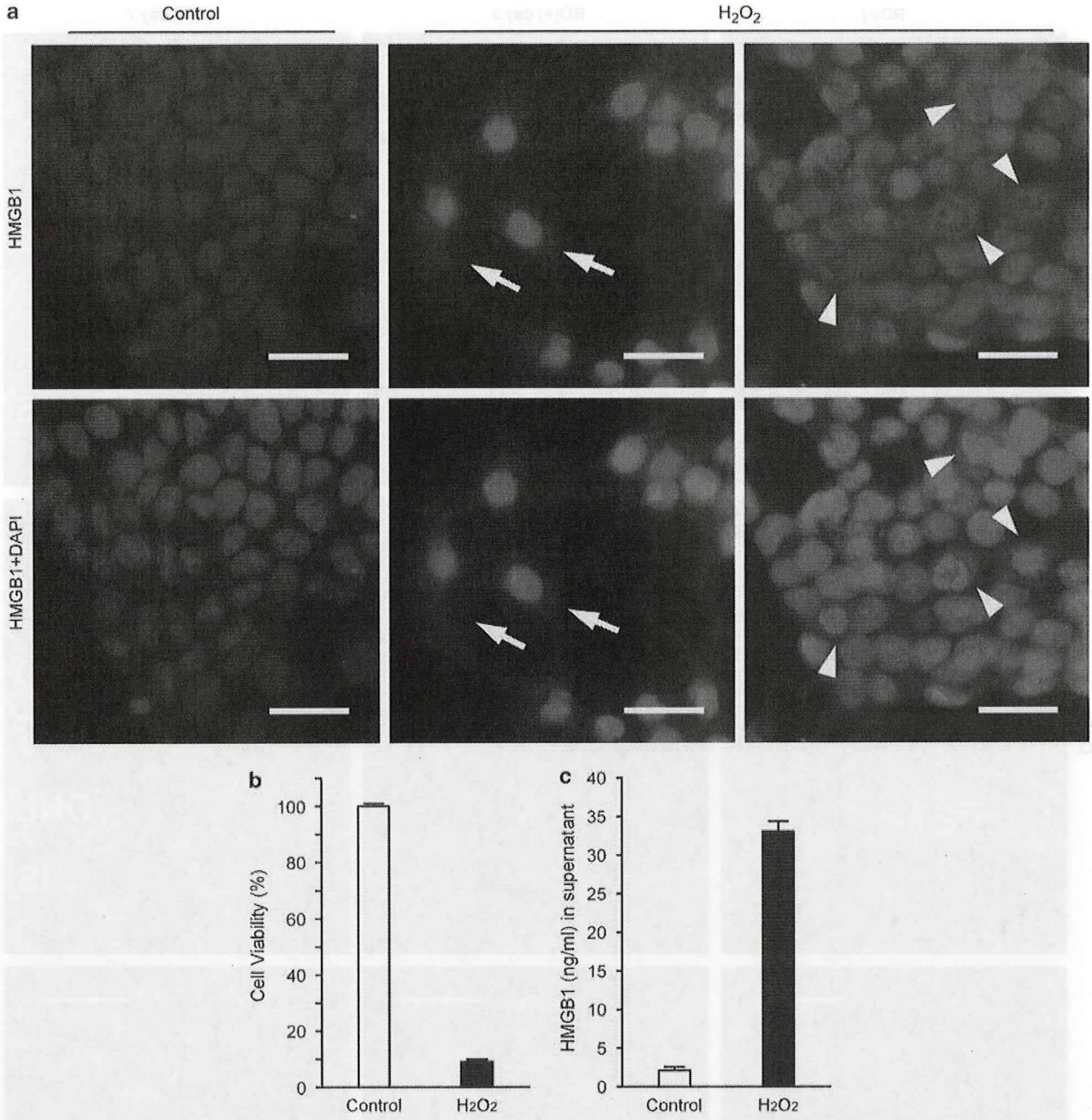

Figure 1 Release of HMGB1 from R28 retinal neuronal cells exposed to excessive oxidative stress. (**a**) Immunofluorescence was performed with anti-HMGB1 antibody (red) and DAPI (blue). HMGB1 is predominantly present in the nuclei of unstimulated R28 cells (left column). Some cells present robust upregulation of HMGB1 in the nuclei, as well as relocation into the cytoplasm (middle column; arrows) on 1 h exposure to a toxic dose of hydrogen peroxide (1 mM). In the other cells, the nuclear HMGB1 is found to be diminished or released into the cytoplasm (right column; arrowheads). Scale bars: 20 μm. (**b**) After 24 h exposure to 1 mM hydrogen peroxide, the cell viability analyzed by MTT assay is decreased to about 10% compared with the control. (**c**) Massive HMGB1 release into the culture supernatant was determined by ELISA after the same treatment as (**b**). The data represent the mean ± s.d. ($n = 3$). Similar results were obtained from three independent experiments.

Figure 2 Immunofluorescence analysis of HMGB1 in a rat model of RD. Representative photomicrographs of retinal sections labeled with anti-HMGB1 antibody (red; **a–c**) and DAPI (blue; **d–f**). Merged images (**g–i**) are also presented. The retinal sections were derived from the control eye (**a, d, g**), those at 3 days (day 3; **b, e, h**), or 7 days after RD (day 7; **c, f, i**). Arrows point to retinal pigment epithelium (**a, g**), and arrowheads indicate subretinal macrophages (**b, c, h, i**). Note that expression of HMGB1 is augmented especially in ONL at day 3 after RD, whereas the upregulation in ONL appears to be subside by day 7 ($n = 6$ for each time point). Scale bars: 50 μm. INL, inner nuclear layer; IS, inner segment; ONL, outer nuclear layer.

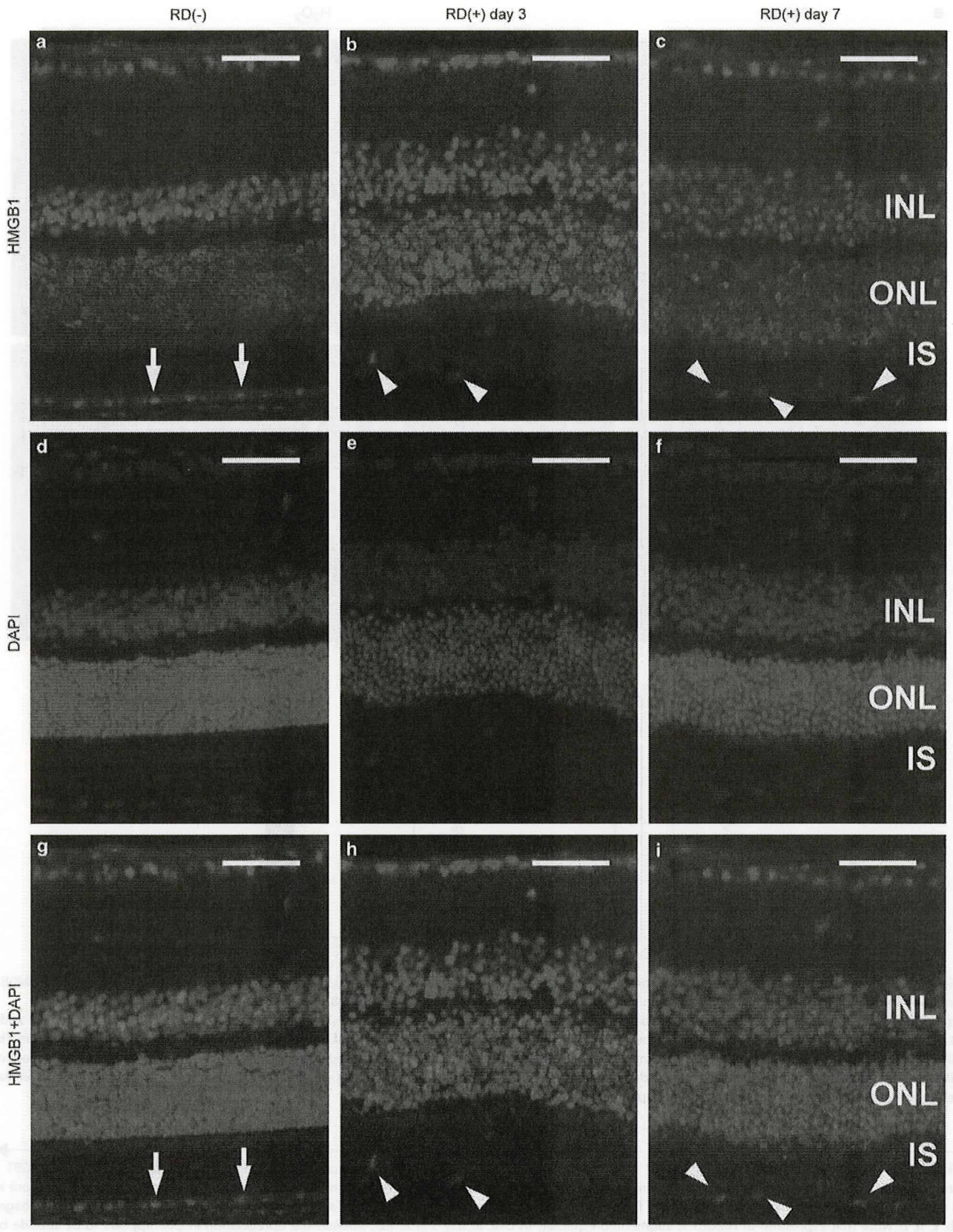
RD(-)
RD(+) day 3
RD(+) day 7
HMGB1
DAPI
HMGB1+DAPI
a
b
c
d
e
f
g
h
i
INL
ONL
IS

reported that macrophages migrated into the subretinal space of this RD model.[32] The migrating macrophages also had abundant HMGB1 expression (Figure 3d, arrowheads), and might have released HMGB1 actively in this space. In line with these data, a large amount of extracellular HMGB1 must be present at least in the subretinal space after RD.

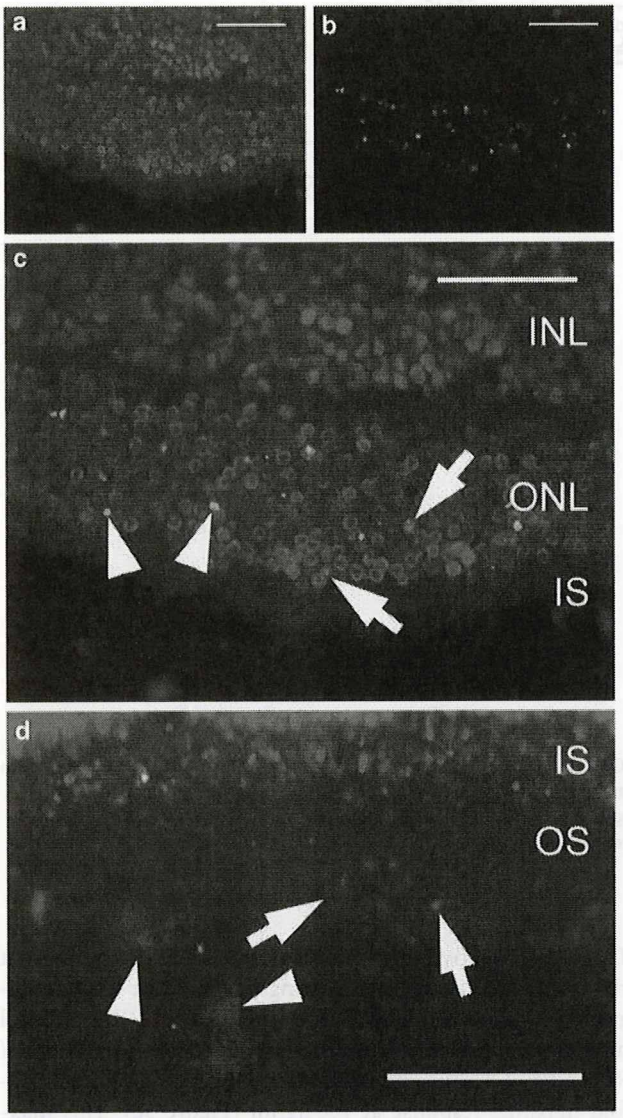

Figure 3 Expression of HMGB1 in DNA-damaged photoreceptors (**a**–**c**) and release of HMGB1 in the subretinal space (**d**). Representative photomicrographs of anti-HMGB1 antibody (red; **a**), TUNEL (green; **b**), and merged image (**c**) from rat retinal sections at 3 days after RD ($n=6$). The early faint TUNEL-positive nuclei (**c**; arrows) have relatively low levels of HMGB1 and the fragmented nuclei (**c**; arrowheads) have almost no apparent HMGB1 immunoreactivity. (**d**) Representative photomicrograph of a merged image of anti-HMGB1 (red), DAPI (blue), and TUNEL (green) obtained from rat retinal sections at 7 days after RD ($n=6$). HMGB1-positive and TUNEL-negative debris (**d**; arrows) and migrating macrophages with abundant HMGB1 expression (**d**; arrowheads) can be observed in the subretinal space. Scale bars: 50 μm. INL, inner nuclear layer; IS, inner segment; ONL, outer nuclear layer; OS, outer segment.

Vitreous HMGB1 and MCP-1 Levels in Patients with RD

The result obtained from the rat model of RD is the first evidence to our knowledge that HMGB1 is involved in RD-induced photoreceptor degeneration. Next, we tested whether extracellular HMGB1 could also be detected in human vitreous samples of RD. Samples were harvested from 35 eyes with RD, including rhegmatogenous RD, RD with macular hole, and atopic RD and 19 eyes with control diseases, including idiopathic epiretinal membrane and idiopathic macular hole (Table 1). The vitreous HMGB1 and MCP-1 levels were significantly higher in the eyes with RD than in those with control diseases (Figure 4). The median HMGB1 level was 1.4 ng/ml (range, 0–28.3) in the eyes with RD and 0.6 ng/ml (range, 0–1.3) in those with control diseases ($P<0.001$; Figure 4a). The median MCP-1 level was 1383.2 pg/ml (range, 39.8–5436.1) in the RD eyes and 404.4 pg/ml (range, 17.9–1168.9) in the control eyes ($P<0.0001$; Figure 4b). The vitreous concentration of HMGB1 was correlated significantly with that of MCP-1 in the 35 eyes with RD by a simple linear regression ($r=0.593$, $P<0.001$; Figure 4c) and by Spearman's rank correlation coefficient ($r=0.613$, $P<0.001$). On the other hand, there was no significant relationship between the vitreous concentrations of HMGB1 and MCP-1 in the 19 eyes of control patients (data not shown). Although there was no significant difference, the HMGB1 levels in the eyes with proliferative vitreoretinopathy (PVR), a condition of retinal fibrosis that follows severe long-standing RD, tended to be lower than those without PVR (Figure 4d). These findings showed that HMGB1 could be released not only in the subretinal space but also in the vitreous cavity after RD-induced photoreceptor degeneration, and that the HMGB1 release was coincident with vitreous MCP-1 expression.

Table 1 Characteristics of the patients

Characteristics	Retinal detachment ($n=35$)	Control diseases ($n=19$)
Age (years)	57.3 ± 16.3	68.2 ± 8.7
Female sex, no. (%)	19 (54)	10 (53)
Patients with PVR, no. (%)	6 (17)	—
Subgroups, no. (%)		
Rhegmatogenous retinal detachment	28 (80)	—
Retinal detachment with macular hole	5 (14)	—
Atopic retinal detachment	2 (6)	—
Idiopathic epiretinal membrane	—	7 (37)
Idiopathic macular hole	—	12 (63)

PVR, proliferative vitreoretinopathy.
Values are expressed as mean ± s.d. Dashes denote not applicable.

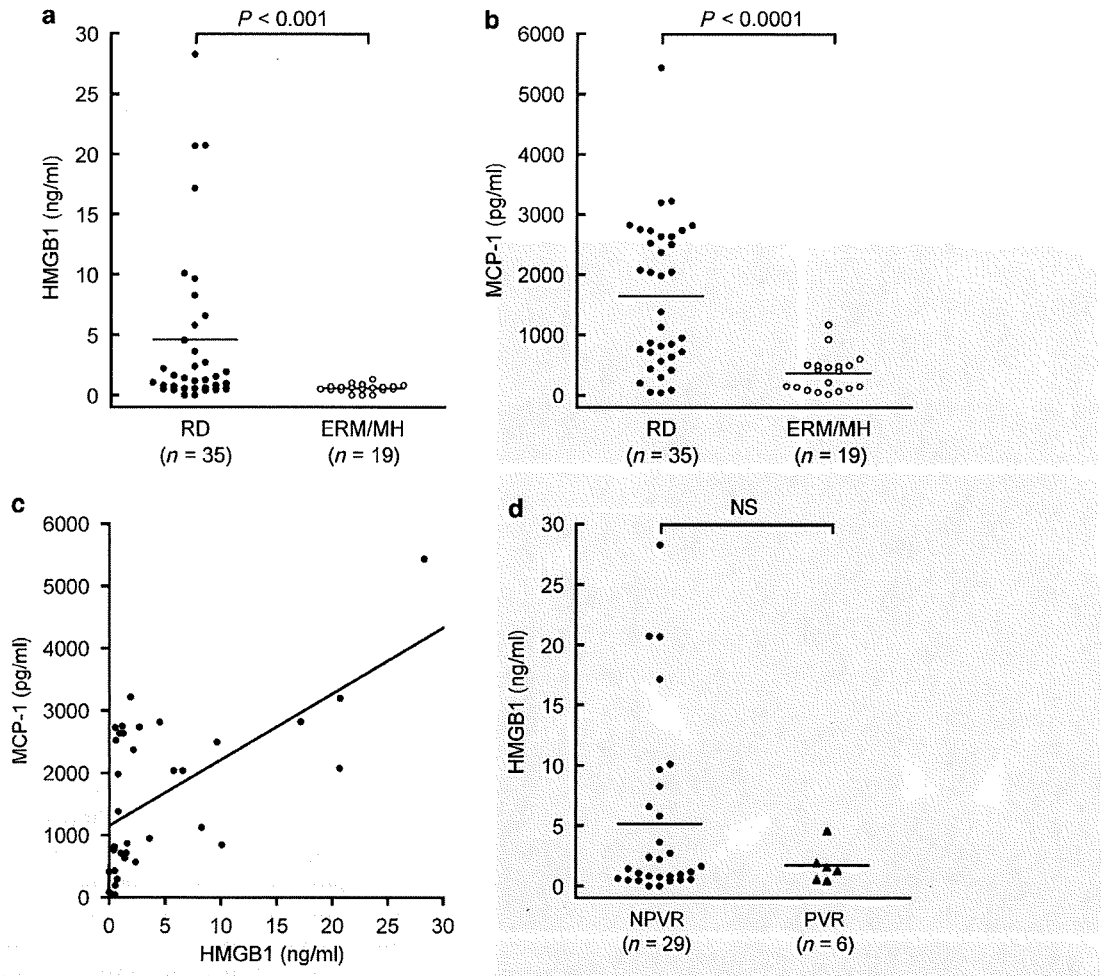

Figure 4 Vitreous levels of HMGB1 and MCP-1. The vitreous HMGB1 (**a**) and MCP-1 (**b**) levels are significantly higher in eyes with RD than in those with control diseases (idiopathic epiretinal membrane or idiopathic macular hole). Each bar indicates the average value. (**c**) Scatter plot for the correlation between vitreous levels of HMGB1 and MCP-1 in eyes with RD (simple linear regression, $r=0.593$, $P<0.001$; Spearman's rank correlation coefficient, $r=0.613$, $P<0.001$). (**d**) The HMGB1 levels in the eyes with PVR tend to be lower than those without PVR. ERM/MH, epiretinal membrane/macular hole; NPVR, no PVR; PVR, proliferative vitreoretinopathy.

RPE Cells Respond Chemotactically to Extracellular HMGB1 through an ERK-Dependent Mechanism

Previous reports have shown that extracellular HMGB1 is a chemoattractant for a variety of cell types.[21,33,34] We investigated whether HMGB1 is also a chemoattractant for RPE cells. Extracellular HMGB1 has been reported to engage multiple receptors, including the receptor for advanced glycation end products (RAGE) and Toll-like receptors 2 and 4.[2,4] In particular, RAGE has been thought to be a crucial receptor for HMGB1-induced cell migration through ERK activation.[33] The expression of RAGE at the RNA and protein level was identified in human RPE[35] and ARPE-19 cells[36,37] in previous studies. It was also shown that the expression of RAGE and HMGB1 was colocalized in the proliferative membrane from an eye with proliferative retinal disease.[38] We, therefore, performed a migration assay using modified Boyden chambers with various concentrations of rHMGB1. The representative photographs in Figure 5 show that rHMGB1 was capable of inducing a significant level of migration (Figure 5b) above that obtained with the control medium (Figure 5a). HMGB1 stimulated the migration of RPE cells in a concentration-dependent manner with a 2.7-fold maximal response at 100 ng/ml (Figure 5c). This maximal response to rHMGB1 was slightly stronger than that induced by rMCP-1 (10 ng/ml). Next, we investigated whether HMGB1 induced phosphorylation of ERK-1/2 in ARPE-19 cells; we stimulated cells with 100 ng/ml rHMGB1 for various time periods and used western blotting with an anti-phospho-ERK-1/2 antibody on whole-cell lysates (Figure 6a). Little phosphorylation of ERK-1/2 could be observed in unstimulated ARPE-19 (at 0 min), but a prominent increase was detected after 5 min of stimulation with rHMGB1. Figure 6a shows that phosphorylation of ERK-1/2 was augmented from 5 to 60 min after rHMGB1 stimulation in comparison

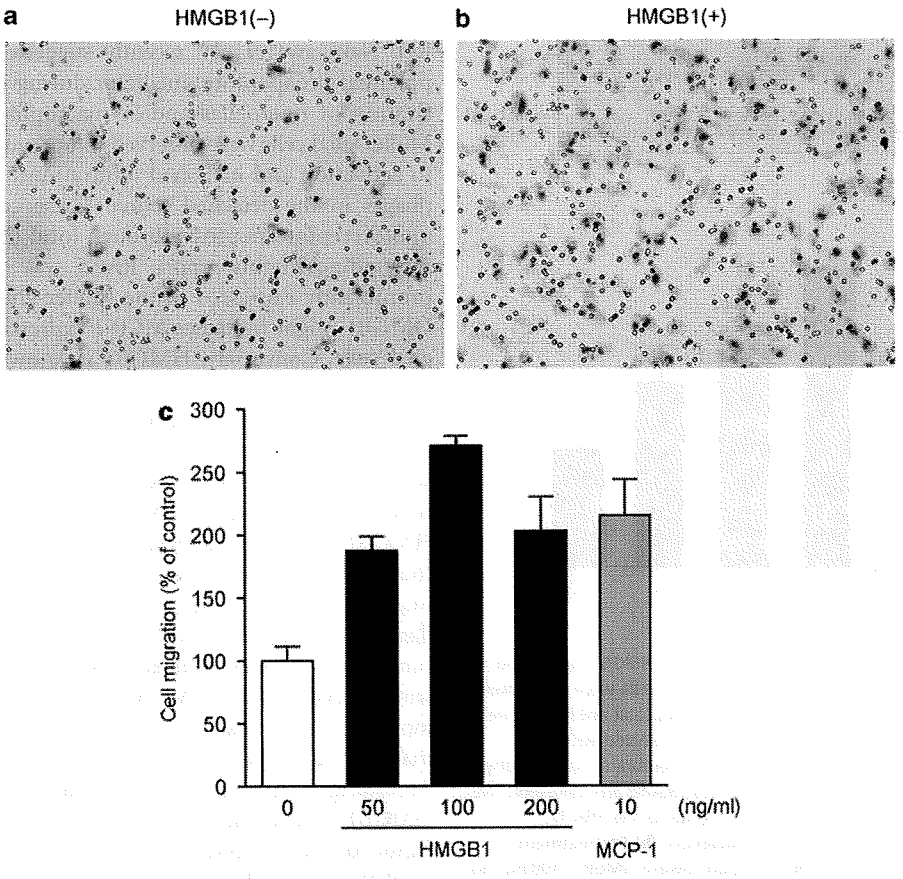

Figure 5 RPE cells migrate in response to HMGB1. Representative photographs of ARPE-19 cells stained with Diff-Quick after migration toward control medium (**a**) or 100 ng/ml HMGB1 (**b**). Original magnification: × 100. (**c**) HMGB1 stimulated ARPE-19 cell migration in a concentration-dependent manner with a 2.7-fold maximal response at 100 ng/ml. The data represent the mean ± s.d. ($n = 3$). All treatments increase the migratory response relative to the control ($P < 0.01$ in Student's *t*-test). Similar results were obtained from three independent experiments.

with unstimulated ARPE-19 (time 0). To demonstrate that the ERK signaling induced by HMGB1 was in fact linked to the migration of RPE cells, we next inhibited ERK-1/2 and assessed cell migration to HMGB1. Pretreatment of ARPE-19 with U0126 abrogated the migration toward rHMGB1 (Figure 6b). Thus, the ERK pathway appears to play an essential role in HMGB1-induced RPE cell migration.

DISCUSSION

Our findings suggest a possible role of HMGB1 in RD, as an essential nuclear protein and a principal danger signal for photoreceptor degeneration. Using an *in vitro* assay of retinal cell death induced by excessive oxidative stress, we found that HMGB1 was augmented in the nucleus by the stress and released into the extracellular space during cell death. On the basis of immunohistochemical analyses of a rat model of RD-induced photoreceptor degeneration, augmentation of HMGB1 in the nucleus is also observed *in vivo* and appears to be crucial for the proper transcription of photoreceptors after RD. Moreover, double labeling with TUNEL reveals defects of upregulation of the nuclear HMGB1 in the DNA-damaged photoreceptors, which are presumably programmed dying photoreceptors. Therefore, we propose that the nuclear HMGB1 in the retinal cells might be critical for retinal cell survival under death stresses both in the *in vivo* RD and *in vitro* retinal cell death. These results for ocular HMGB1 are compatible with previous reports that HMGB1 is a vital nuclear protein and has a protective role in the nucleus.[2,4]

In a previous animal study, Erickson *et al*[17] reported that a loss of photoreceptors in a cat model of RD occurred due to necrosis. During studies on RD, photoreceptor degeneration after RD had been thought to be mainly caused by apoptosis.[15,16] Hisatomi *et al*[32] demonstrated the presence of apoptotic debris in the subretinal space of rat RD. In the present study, considering our immunohistochemistry results from the same rat model of RD, so-called necrotic debris, which is HMGB1 positive and TUNEL negative, was found to be present. On the basis of the previous finding of the preferential release of HMGB1 from necrotic cells,[6] this suggests that necrosis might still be a fundamental type of photoreceptor cell death after RD.

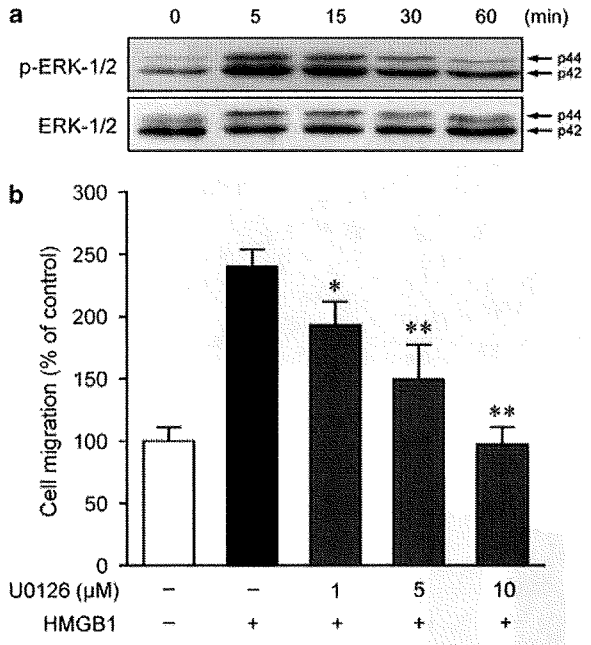

Figure 6 The phosphorylation of ERK is induced by HMGB1 and linked to HMGB1-induced migration of RPE cells. (**a**) ARPE-19 cells were stimulated with HMGB1 (100 ng/ml) for 5, 15, 30, or 60 min, and total cell lysates were analyzed by western blot. ERK-1/2 activation was detected with anti-phospho-ERK-1/2 antibody (p-ERK-1/2). Stripped membrane was reprobed with the antibody against total ERK-1/2 (ERK-1/2). Results are representative of three independent experiments. HMGB1 augments the ERK-1/2 phosphorylation from 5 to 60 min after stimulation. (**b**) Pretreatment of ARPE-19 with U0126 inhibits the cell migration toward HMGB1 (100 ng/ml) in a dose-dependent manner. The data represent the mean ± s.d. ($n = 3$). Similar results were obtained from three independent experiments. $^*P < 0.05$, $^{**}P < 0.01$, compared with vehicle-treated control.

Furthermore, exploring human vitreous samples by ELISA, we found that both HMGB1 and MCP-1 are increased significantly in eyes with RD. Although MCP-1 is a well-known mediator for RD,[39] to our knowledge, this is the first report indicating that extracellular HMGB1 might also be of relevance to human RD. HMGB1 concentration tended to be high in the eye without PVR, but not so with PVR. One possible explanation for this tendency is that HMGB1 might be sequestered and/or masked in PVR, the advanced stage of RD. HMGB1 binds tightly to heparin and proteoglycans with heparan sulfate,[5] and it is also reported that such proteoglycans are abundantly present as the ocular extracellular matrix, even in RD.[40] Hence, these molecules might affect the HMGB1 concentration in the vitreous humor. Nevertheless, this possibility does not negate the presence of HMGB1. Considering the results obtained with the rat RD model, extracellular HMGB1 could be present at much higher levels, at least in the subretinal fluid of RD, and it might serve as a persistent signal adhering to the local damaged retina and/or surrounding matrix as previously described.[5]

It is also of importance that HMGB1 is significantly correlated with MCP-1 in RD vitreous. The secretion of MCP-1 might parallel the extent of photoreceptor degeneration of RD. Nakazawa *et al*[20] recently suggested that MCP-1 is a potential proapoptotic mediator during RD through the activation of microglias and/or macrophages. In their study, Müller-glial cells were observed to upregulate MCP-1, leading to activation and increased infiltration of microglias/macrophages in the detached retina. These cells induced further photoreceptor apoptosis through local oxidative stress. Corresponding to this report, RAGE was also reported to be prominently expressed in the Müller-glial cells.[41] Therefore, HMGB1 might influence MCP-1 expression through Müller-glial cells. Conversely, HMGB1 is known to be released by activated monocytes/macrophages.[7] MCP-1 is a potent stimulator and chemoattractant for monocytes/macrophages,[42] and these cells were observed in the subretinal space of RD with abundant HMGB1 expression. This would also be another possible explanation for the parallel increases of HMGB1 and MCP-1. Nevertheless, the positive correlation of these molecules indicates that cell death-related mediators might be highly orchestrated in ocular degenerative tissue damage. Several studies suggest that extracellular HMGB1 can aggravate tissue damage in neuronal tissues.[10,43] In these studies, extracellular HMGB1 plays a key role in the development of neuronal injury through the induction of inflammation, microglial activation, and neuronal excitotoxicity. According to these recent reports, the presence of extracellular HMGB1 concomitantly with MCP-1 is a possible deteriorating factor for RD, in spite of its essential role in the nucleus.

PVR is one of the most threatening complications of RD. It is thought to be a reactive process to retinal injury, in other words, it is one of the wound-healing responses in the eye. RPE cells are known to be detectable in the fibrotic proliferative membranes of PVR, and play an important role in the pathogenesis of PVR.[44] Thus, the effects of a molecule on PVR formation could be traced to RPE migration, at least in part. Here, we demonstrate that extracellular HMGB1 promotes RPE cell migration by chemotaxis *in vitro*. This result is consistent with previous reports of HMGB1-induced cell migration in various cell types, such as smooth muscle cells,[21,33] fibroblasts,[45] and chondrocytes.[34] We also found that HMGB1 activated phosphorylation of ERK-1/2 in RPE cells and the migration induced by HMGB1 was dependent on ERK phosphorylation. The phosphorylation of ERK is associated with cell proliferation and cell migration through effects on cell–matrix contacts.[46] It was also reported to be found in Müller-glial cells after RD.[47] Taken together, our results suggest that extracellular HMGB1 from dying ocular cells might affect retinal cells through ERK phosphorylation and potentially serve to promote the formation of PVR, which is wound healing, but has a pathological meaning in the eye. Several new strategies for prevention of ocular fibrosis, especially targeting specific signaling pathways, have been proven to be beneficial in animal models.[48–50] We propose that the identification and further characterization of danger signals, including HMGB1, would provide a novel

perspective for better understanding the molecular pathogenesis of PVR before applying these promising therapeutic manipulations to human subjects.

It has been suggested that post-transcriptional modifications of HMGB1, such as acetylation, methylation, and phosphorylation, might influence its activity.[51] Some recent reports also demonstrate that the proinflammatory activity of HMGB1 is due to combined action with other molecules.[52] The present data are mostly limited to the presence of HMGB1 rather than its biological activity, and we do not address what modifications or molecules are involved in intraocular HMGB1. However, we identify for the first time that HMGB1 is evident in a typical retinal injury of human RD, in which nuclear HMGB1 is a crucial nuclear protein and extracellular HMGB1 is a danger signal that might be required for the ocular wound-healing response. Our findings might have relevance for the underlying mechanisms of degenerative neuronal diseases. Further detailed studies will be needed to obtain more accurate knowledge and therapeutic value of HMGB1 in human diseases.

ACKNOWLEDGEMENTS

We thank Dr GM Siegel, The State University of New York, for providing R28 cells; Drs Takashi Ito, Yoko Oyama, Toshiaki Shimizu, Kazunori Takenouchi, Kiyoshi Kikuchi, Masahiro Iwata, Yuko Nawa, Yoko Morimoto, Naoki Miura, and Noboru Taniguchi for their helpful advice and technical support; Miss Nobue Uto, Tomoka Nagasato, Hisayo Sameshima, and Maiko Yamaguchi for their assistance with the experiments. This research was supported in part by a grant from the Research Committee on Chorioretinal Degeneration and Optic Atrophy, Ministry of Health, Labor, and Welfare and by a grant-in-aid for Scientific Research from the Ministry of Education, Science, and Culture of the Japanese Government.

1. Bianchi ME. DAMPs, PAMPs and alarmins: all we need to know about danger. J Leukoc Biol 2007;81:1–5.
2. Ulloa L, Messmer D. High-mobility group box 1 (HMGB1) protein: friend and foe. Cytokine Growth Factor Rev 2006;17:189–201.
3. Martin P. Wound healing—aiming for perfect skin regeneration. Science 1997;276:75–81.
4. Lotze MT, Tracey KJ. High-mobility group box 1 protein (HMGB1): nuclear weapon in the immune arsenal. Nat Rev Immunol 2005;5: 331–342.
5. Huttunen HJ, Rauvala H. Amphoterin as an extracellular regulator of cell motility: from discovery to disease. J Intern Med 2004;255:351–366.
6. Scaffidi P, Misteli T, Bianchi ME. Release of chromatin protein HMGB1 by necrotic cells triggers inflammation. Nature 2002;418:191–195.
7. Wang H, Bloom O, Zhang M, *et al.* HMG-1 as a late mediator of endotoxin lethality in mice. Science 1999;285:248–251.
8. Passalacqua M, Patrone M, Picotti GB, *et al.* Stimulated astrocytes release high-mobility group 1 protein, an inducer of LAN-5 neuroblastoma cell differentiation. Neuroscience 1998;82:1021–1028.
9. Ito T, Kawahara K, Nakamura T, *et al.* High-mobility group box 1 protein promotes development of microvascular thrombosis in rats. J Thromb Haemost 2007;5:109–116.
10. Kim JB, Sig Choi J, Yu YM, *et al.* HMGB1, a novel cytokine-like mediator linking acute neuronal death and delayed neuroinflammation in the postischemic brain. J Neurosci 2006;26:6413–6421.
11. Campana L, Bosurgi L, Rovere-Querini P. HMGB1: a two-headed signal regulating tumor progression and immunity. Curr Opin Immunol 2008;20:518–523.
12. Inoue K, Kawahara K, Biswas KK, *et al.* HMGB1 expression by activated vascular smooth muscle cells in advanced human atherosclerosis plaques. Cardiovasc Pathol 2007;16:136–143.
13. Taniguchi N, Kawahara K, Yone K, *et al.* High mobility group box chromosomal protein 1 plays a role in the pathogenesis of rheumatoid arthritis as a novel cytokine. Arthritis Rheum 2003;48:971–981.
14. Morimoto Y, Kawahara KI, Tancharoen S, *et al.* Tumor necrosis factor-alpha stimulates gingival epithelial cells to release high mobility-group box 1. J Periodontal Res 2008;43:76–83.
15. Cook B, Lewis GP, Fisher SK, *et al.* Apoptotic photoreceptor degeneration in experimental retinal detachment. Invest Ophthalmol Vis Sci 1995;36:990–996.
16. Arroyo JG, Yang L, Bula D, *et al.* Photoreceptor apoptosis in human retinal detachment. Am J Ophthalmol 2005;139:605–610.
17. Erickson PA, Fisher SK, Anderson DH, *et al.* Retinal detachment in the cat: the outer nuclear and outer plexiform layers. Invest Ophthalmol Vis Sci 1983;24:927–942.
18. Vazquez-Chona F, Song BK, Geisert Jr EE. Temporal changes in gene expression after injury in the rat retina. Invest Ophthalmol Vis Sci 2004;45:2737–2746.
19. Arimura N, Ki IY, Hashiguchi T, *et al.* High-mobility group box 1 protein in endophthalmitis. Graefes Arch Clin Exp Ophthalmol 2008;246: 1053–1058.
20. Nakazawa T, Hisatomi T, Nakazawa C, *et al.* Monocyte chemoattractant protein 1 mediates retinal detachment-induced photoreceptor apoptosis. Proc Natl Acad Sci USA 2007;104:2425–2430.
21. Porto A, Palumbo R, Pieroni M, *et al.* Smooth muscle cells in human atherosclerotic plaques secrete and proliferate in response to high mobility group box 1 protein. FASEB J 2006;20:2565–2566.
22. Hisatomi T, Sakamoto T, Murata T, *et al.* Relocalization of apoptosis-inducing factor in photoreceptor apoptosis induced by retinal detachment *in vivo*. Am J Pathol 2001;158:1271–1278.
23. Neekhra A, Luthra S, Chwa M, *et al.* Caspase-8, -12, and -3 activation by 7-ketocholesterol in retinal neurosensory cells. Invest Ophthalmol Vis Sci 2007;48:1362–1367.
24. Biswas KK, Sarker KP, Abeyama K, *et al.* Membrane cholesterol but not putative receptors mediates anandamide-induced hepatocyte apoptosis. Hepatology 2003;38:1167–1177.
25. Hoppe G, Rayborn ME, Sears JE. Diurnal rhythm of the chromatin protein Hmgb1 in rat photoreceptors is under circadian regulation. J Comp Neurol 2007;501:219–230.
26. Hinton DR, He S, Graf K, *et al.* Mitogen-activated protein kinase activation mediates PDGF-directed migration of RPE cells. Exp Cell Res 1998;239:11–15.
27. Han QH, Hui YN, Du HJ, *et al.* Migration of retinal pigment epithelial cells *in vitro* modulated by monocyte chemotactic protein-1: enhancement and inhibition. Graefes Arch Clin Exp Ophthalmol 2001;239:531–538.
28. Glotin AL, Calipel A, Brossas JY, *et al.* Sustained versus transient ERK1/2 signaling underlies the anti- and proapoptotic effects of oxidative stress in human RPE cells. Invest Ophthalmol Vis Sci 2006;47: 4614–4623.
29. Klein JA, Ackerman SL. Oxidative stress, cell cycle, and neurodegeneration. J Clin Invest 2003;111:785–793.
30. Tang D, Shi Y, Kang R, *et al.* Hydrogen peroxide stimulates macrophages and monocytes to actively release HMGB1. J Leukoc Biol 2007;81:741–747.
31. Hollborn M, Francke M, Iandiev I, *et al.* Early activation of inflammation- and immune response-related genes after experimental detachment of the porcine retina. Invest Ophthalmol Vis Sci 2008;49: 1262–1273.
32. Hisatomi T, Sakamoto T, Sonoda KH, *et al.* Clearance of apoptotic photoreceptors: elimination of apoptotic debris into the subretinal space and macrophage-mediated phagocytosis via phosphatidylserine receptor and integrin alphavbeta3. Am J Pathol 2003;162:1869–1879.
33. Degryse B, Bonaldi T, Scaffidi P, *et al.* The high mobility group (HMG) boxes of the nuclear protein HMG1 induce chemotaxis and cytoskeleton reorganization in rat smooth muscle cells. J Cell Biol 2001;152:1197–1206.
34. Taniguchi N, Yoshida K, Ito T, *et al.* Stage-specific secretion of HMGB1 in cartilage regulates endochondral ossification. Mol Cell Biol 2007;27:5650–5663.
35. Yamada Y, Ishibashi K, Ishibashi K, *et al.* The expression of advanced glycation endproduct receptors in rpe cells associated with basal deposits in human maculas. Exp Eye Res 2006;82: 840–848.

36. Howes KA, Liu Y, Dunaief JL, *et al.* Receptor for advanced glycation end products and age-related macular degeneration. Invest Ophthalmol Vis Sci 2004;45:3713–3720.
37. Ma W, Lee SE, Guo J, *et al.* RAGE ligand upregulation of VEGF secretion in ARPE-19 cells. Invest Ophthalmol Vis Sci 2007;48: 1355–1361.
38. Pachydaki SI, Tari SR, Lee SE, *et al.* Upregulation of RAGE and its ligands in proliferative retinal disease. Exp Eye Res 2006;82: 807–815.
39. Elner SG, Elner VM, Jaffe GJ, *et al.* Cytokines in proliferative diabetic retinopathy and proliferative vitreoretinopathy. Curr Eye Res 1995;14:1045–1053.
40. Wang JB, Tian CW, Guo CM, *et al.* Increased levels of soluble syndecan-1 in the subretinal fluid and the vitreous of eyes with rhegmatogenous retinal detachment. Curr Eye Res 2008;33:101–107.
41. Barile GR, Pachydaki SI, Tari SR, *et al.* The RAGE axis in early diabetic retinopathy. Invest Ophthalmol Vis Sci 2005;46: 2916–2924.
42. Matsushima K, Larsen CG, DuBois GC, *et al.* Purification and characterization of a novel monocyte chemotactic and activating factor produced by a human myelomonocytic cell line. J Exp Med 1989;169:1485–1490.
43. Pedrazzi M, Raiteri L, Bonanno G, *et al.* Stimulation of excitatory amino acid release from adult mouse brain glia subcellular particles by high mobility group box 1 protein. J Neurochem 2006;99:827–838.
44. Pastor JC, de la Rua ER, Martin F. Proliferative vitreoretinopathy: risk factors and pathobiology. Prog Retin Eye Res 2002;21:127–144.
45. Straino S, Di Carlo A, Mangoni A, *et al.* High-mobility group box 1 protein in human and murine skin: involvement in wound healing. J Invest Dermatol 2008;128:1545–1553.
46. Lawrence MC, Jivan A, Shao C, *et al.* The roles of MAPKs in disease. Cell Res 2008;18:436–442.
47. Nakazawa T, Takeda M, Lewis GP, *et al.* Attenuated glial reactions and photoreceptor degeneration after retinal detachment in mice deficient in glial fibrillary acidic protein and vimentin. Invest Ophthalmol Vis Sci 2007;48:2760–2768.
48. Saika S. TGFbeta pathobiology in the eye. Lab Invest 2006;86 :106–115.
49. Saika S, Yamanaka O, Nishikawa-Ishida I, *et al.* Effect of Smad7 gene overexpression on transforming growth factor beta-induced retinal pigment fibrosis in a proliferative vitreoretinopathy mouse model. Arch Ophthalmol 2007;125:647–654.
50. Saika S, Yamanaka O, Sumioka T, *et al.* Fibrotic disorders in the eye: targets of gene therapy. Prog Retin Eye Res 2008;27:177–196.
51. Bianchi ME, Manfredi AA. High-mobility group box 1 (HMGB1) protein at the crossroads between innate and adaptive immunity. Immunol Rev 2007;220:35–46.
52. Sha Y, Zmijewski J, Xu Z, *et al.* HMGB1 develops enhanced proinflammatory activity by binding to cytokines. J Immunol 2008;180:2531–2537.

Posturing Time after Macular Hole Surgery Modified by Optical Coherence Tomography Images: A Pilot Study

KYOKO MASUYAMA, KEITA YAMAKIRI, NOBORU ARIMURA, YASUSHI SONODA, NORIHITO DOI, AND TAIJI SAKAMOTO

• PURPOSE: To see the early postoperative stage of macular hole (MH) surgery and to distinguish eyes needing prolonged posturing from those that do not use Fourier-domain optical coherence tomography (FD-OCT).
• DESIGN: Interventional case series.
• METHODS: Sixteen eyes of 15 patients with MH underwent the protocol at Kagoshima University Hospital. After the pars plana vitrectomy with 16% SF_6 gas tamponade followed by posturing, the eyes were examined by FD OCT from 3 hours to the day after surgery. After MH closure was confirmed, posturing was stopped. Follow-up was performed for 4 months or longer. The main outcome measures included time and OCT finding of MH closure after surgery.
• RESULTS: On the day after surgery, the macula could be examined by FD-OCT in 13 of 16 eyes; 10 eyes had a closed MH and 3 had an unclosed MH. At day 2, 2 of the 3 eyes with unclosed MHs on day 1 demonstrated a closed MH. Posturing continued for 8 days in 4 eyes whose MH closure was not confirmed. The MH was closed in all eyes within 1 month. FD-OCT showed bridge formation of the neural retina in 9 eyes and simple closure in 3 eyes within 7 days. At 1 month, 12 eyes showed simple closure and 4 eyes showed bridge formation. Among 9 eyes with bridge formation within 7 days, 6 eyes had changed to simple closure at 1 month.
• CONCLUSIONS: FD-OCT enabled confirmation of MH closure the day after surgery even in gas-filled eyes. This imaging method may be a good indicator to determine when to stop posturing for each patient. (Am J Ophthalmol 2009;147:481–488. © 2009 by Elsevier Inc. All rights reserved.)

SINCE KELLY AND WENDEL'S REPORT, IDIOPATHIC macular hole (MH) has become a treatable disease, and the recent anatomic success rate of MH closure is more than 90%.[1–6] Despite such a high success rate, there is still much room for improvement with this treatment. For example, the requirement for prolonged face-down posturing is a major burden on patients and physicians.[7,8]

Since Tornambe and associates' challenge, there has been a trend to shorten the period of posturing.[9–18] Some authors report that 1 day of posturing is equivalent to 1 week of posturing,[10] and other reports show that air tamponade followed by shorter posturing is equally effective for MH closure as is a long period of gas tamponade with prolonged posturing.[7,17] However, there are still concerns that shorter posturing may cause MH surgery to fail in some eyes, whereas prolonged posturing may cause most patients needless suffering. Therefore, a tailor-made postoperative program would be much more desirable rather than the uniform program largely followed now.

To devise a personally based approach, it is essential to monitor the very early stage of the MH closing process after surgery, especially during the gas-filled period; however, only a few studies have documented this process at the very early phase of the postoperative period. Takahashi and Kishi reported 2 closure patterns, bridge formation or simple closure, in the early phase after surgery using optical coherence tomography (OCT).[19] However, their observations were made 1 month after surgery, which did not reflect the very early phase of MH closure, and the information is not necessarily helpful for determining the duration of posturing. More recently, Hasler and Prünte showed OCT findings for 2 eyes on the first postoperative day through vitreous humor, but not gas-filling.[17]

Optical coherence tomography has made a great contribution to determining retinal pathologic features, including MH.[20–26] Nonetheless, the very early phase of MH closure after surgery cannot be observed in detail even with conventional (time-domain [TD]) OCT. One of the reasons is that clear imaging is hampered by a strong light reflex from the posterior surface in a gas-filled eye. Another reason is that TD-OCT cannot identify the macular area accurately in a gas-filled eye. Although no hole was found in the section of the possible macular area, this does not always mean the MH is closed, because the exact macula is not identifiable by TD-OCT. In contrast, Fourier-domain OCT (FD-OCT) has a function to scan a broad area within a short period, and serial scanning of a broad area allows more accurate identification and examination of the macula.[23]

In this study, the very early phase of the MH closure process was investigated using FD-OCT in eyes with full

Accepted for publication Sep 24, 2008.
Department of Ophthalmology, Kagoshima University Graduate School of Medical and Dental Sciences, Kagoshima, Japan.
Inquiries to Taiji Sakamoto, Department of Ophthalmology, Kagoshima University Graduate School of Medical and Dental Sciences, 8-35-1 Sakuragaoka, Kagoshima 890-8520, Japan; e-mail: tsakamot@m3.kufm.kagoshima-u.ac.jp

0002-9394/09/$36.00
doi:10.1016/j.ajo.2008.09.028

gas. This information would be important not only for a better understanding of the MH pathologic features, but also for reducing the burden on the patient with little risk through a tailor-made approach.

METHODS

ALL CONSECUTIVE PATIENTS WITH IDIOPATHIC MH WHO agreed to participate in this study from March 1, 2007 through February 29, 2008 were enrolled and a prospective study was performed. Data collected included patient age and gender, MH stage (Gass classification) and latency (judged by clinical history), cataract grade of mild (nuclear sclerosis 1+) or moderate to advanced (nuclear sclerosis 2+ or 3+), and Snellen best-corrected visual acuity (BCVA) before and after surgery. Postoperative adverse events such as infectious endophthalmitis, intraocular pressure rise, retinal detachment (RD), vitreous hemorrhage, choroidal detachment, and corneal pathologic features were noted. All surgeries were performed using local or general anesthesia (depending on patient general condition, preference, or both), and a standardized surgical procedure was used. All patients with a phakic eye received phacoemulsification cataract surgery with implantation of an intraocular lens (IOL). A 20-gauge standard pars plana vitrectomy (PPV) was performed, and the internal limiting membrane (ILM) was peeled with the help of triamcinolone (Kenacort-A; Bristol Pharmaceuticals KK, Tokyo, Japan), as in our previously described method.[27,28] After removing residual triamcinolone, the eye was flushed with 16% SF_6 gas and a maximum fill was attempted. All eyes were left firm after surgery with no documented leakage. The patients were postured face down as immediately as possible after surgery. If the patient agreed, the first OCT examination was performed 3 hours after surgery. Otherwise, the first OCT examination was performed every day from the day after surgery. When MH closure was found by OCT, the patients were asked to stop face-down posturing. This meant that the patients could assume any posturing, including during meals and for personal hygiene, although they were advised not to lie flat on their backs at night for 1 week to avoid IOL dislocation. The patients were followed up for 4 months or longer.

• **OPTICAL COHERENCE TOMOGRAPHY EXAMINATION AND DETERMINATION OF THE MACULA:** The posterior retina covering possible macular area was scanned with FD-OCT (Topcon, Tokyo, Japan) using a raster scan program. Using this system, 512 × 170 scans (horizontal × vertical) were possible within the 6 × 6-mm^2 area.[23] Thus, it is unlikely that an unclosed MH was overlooked by this method. MH closure by OCT was defined as no interruption of the internal line of the inner retina in any macular area. If MH closure was confirmed by this method, face-down posturing was discontinued regardless of residual gas in the vitreous cavity.

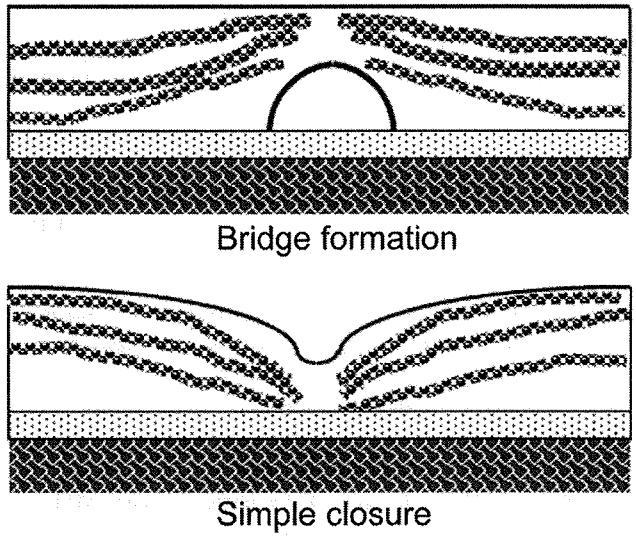

FIGURE 1. Diagrams illustrating optical coherence tomography (OCT) findings after macular hole (MH) surgery. (Top) Bridge formation type. (Bottom) Simple closure type.

Previously, OCT findings of MH at 1 month after surgery were classified as bridging formation or simple closure patterns.[19] Thus, the OCT findings after surgery that are presented herein were classified according to their criteria. Bridge formation type was defined as eyes that showed tissue that was continuous with the inner retina over the retinal pigment epithelium (RPE) that mimicked foveal RD (Figure 1), and simple closure type was defined as eyes that showed a normal foveal configuration from the initial examination.

RESULTS

THE STUDY INCLUDED 16 EYES OF 15 PATIENTS (7 EYES OF 6 females and 9 eyes of 9 male). Age ranged from 54 to 78 years. Preoperative BCVA ranged from 20/400 to 20/30 (mean, 20/200). The possible latency period before surgery ranged from 0 to 9 months. All eyes were phakic. Four eyes had a stage 2 MH (25%), 10 eyes had a stage 3 MH (62.5%), and 2 eyes had a stage 4 MH (12.5%). These are summarized in Table 1. Sizes of MH ranged from 0.15 to 0.4 disc diameter.

Three hours after surgery, 5 eyes were examined by FD-OCT. Three of these eyes showed comparatively clear images to determine MH closure. The remaining 2 eyes did not show interpretable images because of the media opacity. On the day after surgery (day 1), the macular area could be examined by FD-OCT in 13 eyes, whereas it could not be imaged clearly in 3 eyes because of media opacity: 2 eyes because of corneal haziness and 1 eye because of minimal hyphema. Among 13 eyes examined,

TABLE 1. Basic Characteristics of the Patients of Macular Hole Surgery

Case No.	Eye No.	Eye	Age at Onset of MH (yrs)	Gender	MH Stage (Gass Classification)	Preoperative Latency (mos)	MH Size (DD)	Cataract Classification	Preoperative VA	Postoperative (Final) VA (Refraction)	Follow-up (mos)
1	1	Right	72	F	3	9	0.4	+2	20/125	20/100 (−2.50)	4
2	2	Left	57	M	3	2	0.2	+1	20/100	20/63 (−3.50)	5
3	3	Right	57	M	3	2	0.25	+1	20/63	20/20 (−4.50)	7
4	4	Left	55	F	3	1	0.25	+2	20/63	20/25 (−2.25)	7
5	5	Right	54	F	4	3	0.25	+1	20/200	20/63 (−0.75)	7
6	6	Right	69	F	2	4	0.4	+1	20/200	20/100 (−0.75)	6
7	7	Right	67	M	4	1	0.25	+1	20/200	20/32 (−1.25)	6
8	8	Left	78	M	2	3	0.2	+1	20/125	20/16 (−0.75)	4
9	9	Left	74	M	3	2	0.15	+1	20/63	20/16 (−1.00)	4
10	10	Left	60	F	3	1	0.33	+1	20/32	20/16 (−6.75)	5
	11	Right	60	F	3	2	0.33	+1	20/40	20/20 (−0.75)	5
11	12	Left	62	M	2	1	0.4	+2	20/400	20/50 (−0.35)	5
12	13	Left	55	M	3	0 (2 weeks)	0.5	+2	20/50	20/32 (−5.50)	5
13	14	Right	70	M	3	4	0.33	+1	20/200	20/100 (−0.60)	6
14	15	Right	78	M	2	1	0.4	+2	20/200	20/63 (−2.00)	6
15	16	Left	58	F	3	2	0.33	+0.5	20/50	20/25 (−1.25)	4

DD = disc diameter; F = female; M = male; MH = mascular hole; mos = months; VA = visual acuity; yrs = years.
Cataract grade +1, nuclear sclerosis; +2, moderate nuclear sclerosis; +3, advanced sclerosis.

10 eyes showed closed MH and 3 eyes showed unclosed MH. There was a bridge formation on the neural retina over a small amount of subretinal fluid (SRF) on the macular area in 7 eyes. Some of the bridges had a fistula-like structure (Figure 2). Posturing of patients having eyes with closed MH was stopped. On day 2, 2 of 3 eyes with unclosed MH documented by FD-OCT on day 1 were found to have a closed MH. Posturing of these patients then was stopped. From day 3 to day 7, the macular area could not be observed by FD-OCT because of strong light reflex from the lower surface of gas that occupied approximately 70% of the orbit. The volume of gas was reduced to less than 50% of the orbit after 7 days. Consequently, the macular area of all 16 eyes could be examined by FD-OCT, and MH closure was confirmed on day 9. The gas disappeared completely within 14 days in all eyes. At 1 month or later, the macular area could be observed clearly by both biomicroscopy and FD-OCT. Through the observations, no recurrence was found in any eyes.

Within 7 days, OCT-documented patterns of 12 eyes were determined; 3 eyes showed a simple closure pattern and 9 eyes showed a bridge formation pattern. At 1 month, 12 eyes showed a simple closure pattern and 4 eyes showed a bridge formation pattern (Table 2). Among 9 eyes having a bridge formation within 7 days, 6 eyes showed a simple closure pattern at 1 month. In contrast, no eyes with a simple closure pattern within 7 days changed to a bridge formation pattern at 1 month. BCVA improved in every eye. Comparatively worse postoperative BCVA (20/100) was found in those with long latency (4 months or longer). Four eyes with a bridge formation pattern at 1 month showed fair postoperative BCVA (20/63, 20/16, 20/20, and 20/25). There was no clear correlation between postoperative BCVA and any of the following: MH size, stage, and pattern of MH closure.

Two eyes showed transient intraocular pressure rises within 2 weeks after surgery, which were controlled by eye drops. There were no other defined adverse events in any eyes.

• **REPRESENTATIVE CASES:** *Case 10 (eye 11).* A 60-year-old woman noted visual disturbance and metamorphopsia for 2 months in her right eye and was referred to our hospital. Her BCVA was 20/40, and FD-OCT examination showed stage 3 MH of 0.33 disc diameter with parafoveal cystic change (Figure 2). She underwent a standard PPV with phacoemulsification and IOL implantation as described above. Posturing started immediately after surgery. At 3 hours, FD-OCT examination showed that the intraretinal cyst found before surgery was obscure and there was bridging of the neural retina without any MH structure, and the MH was thought to be closed as bridge formation type. On account of this result, the face-down posturing was stopped. The next day, the MH closure also was confirmed clearly by FD-OCT. The intraretinal cyst could not be observed. The fistula-like structure of the neural retinal bridge became evident on the SRF. At 1 month, BCVA improved to 20/20. FD-OCT examination showed a foveal depression with minimal SRF. A slit-like structure in the neural retinal bridge disappeared completely.

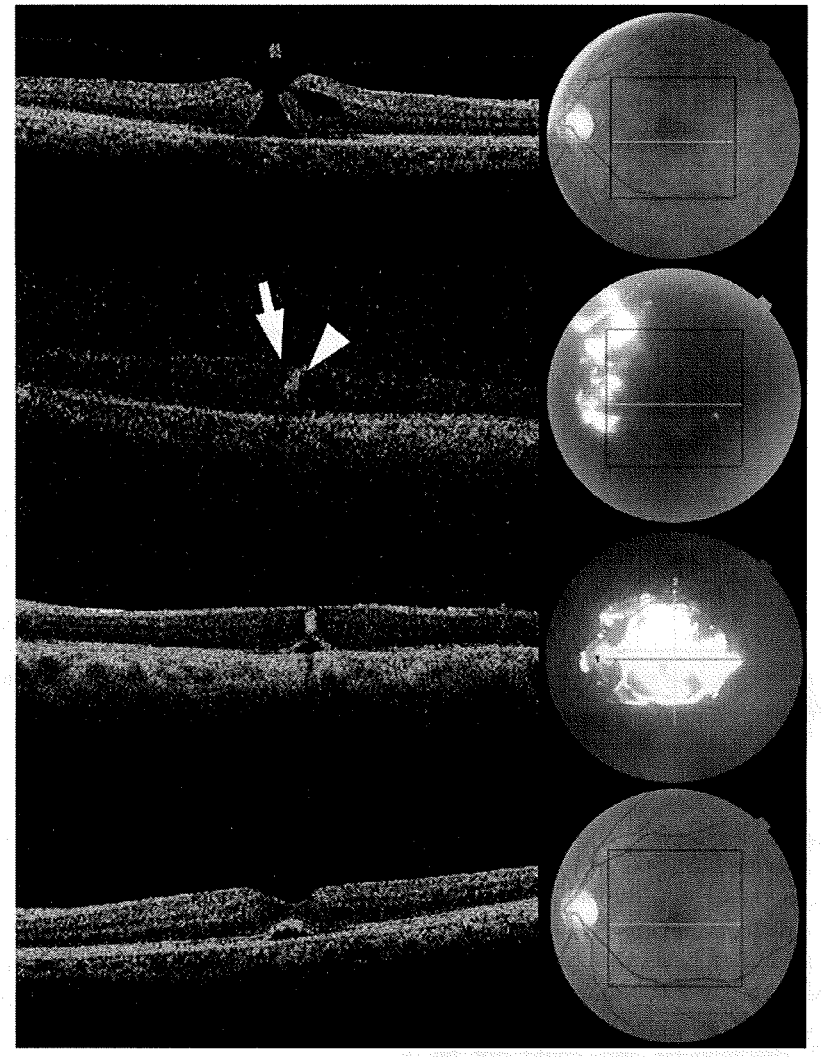

FIGURE 2. Fourier-domain OCT (FD-OCT) images and ocular fundus photographs after MH surgery obtained from Case 10 (eye 11). (Top row) Preoperative stage showing stage 3 MH. (Left) Several intraretinal cysts are found in the perifoveal retina. (Second row) Three hours after surgery. (Left) The inner surface of the retina appears to be continuous across the fovea (arrow). There is a hyperreflex spot on the macula (arrowhead). (Right) A strong light reflex is observed in ocular fundus. (Third row) One day after surgery. (Left) A bridging formation of tissue is found on the possible macular area. A hyperreflex spot also is visible in the retina like a fistula. Subretinal fluid beneath the fovea also is apparent. (Right) A strong light reflex also comes from the posterior retinal surface. (Bottom row) One month after surgery. (Left) MH is closed with foveal depression and subretinal space. (Right) MH disappeared. Square lines in the right figures show the area that was scanned serially by FD-OCT. Yellow or blue single lines also indicate the scanned sections shown on the left images.

Case 12 (eye 13). A 55-year-old male reported visual disturbance in his left eye for 2 weeks' duration. His BCVA was 20/50 at his first visit to our hospital. FD-OCT examination showed a stage 3 MH of 0.25 disc diameter (Figure 3). He also underwent a standard PPV with cataract surgery as described above. Posturing was started immediately after surgery. The next day, FD-OCT was performed and the hole appeared to remain open. At day 2, although the ocular fundus could be seen more clearly, the images by FD-OCT were unchanged. Therefore, posturing was continued for another 5 days until the macular area reappeared below the gas-bubble. During this period, the macular area could not be observed clearly by FD-OCT. FD-OCT at day 8 showed closure of the MH associated with foveal depression. BCVA improved to 20/32 at 5 months.

DISCUSSION

ALTHOUGH THE OCULAR FUNDUS IS OBSERVABLE EVEN in a gas-filled eye by conventional TD-OCT, a detailed examination of the macular area is hampered by a strong light reflex. Kasuga and associates reported that 4 (58%)

TABLE 2. Surgical Results and FD OCT Pattern after Macular Hole Surgeryat Each Time Point

Eye No.	MH Closure Confirmed by FD-OCT						Face-down Posturing Period (days)	Period (days) until Gas decreased to 50%	OCT Pattern	
	Three Hours after Surgery	Day 1 (1 day after surgery)	% of Gas on Day 1	Day 2 (2 days after surgery)	Day 8 (8 days after surgery)	One Month after Surgery			Within 7 days after Surgery	At One Month after Surgery
1	NA	Closed	100	NA	Closed	Closed	1	7	Simple	Simple
2	ND	Unclosed	90	Closed	Closed	Closed	2	6	Bridge	Bridge
3	ND	Unclosed	90	Closed	Closed	Closed	2	6	Bridge	Simple
4	NA	Closed	95	NA	Closed	Closed	1	8	Bridge	Simple
5	NA	Closed	96	NA	Closed	Closed	1	6	Bridge	Simple
6	NA	Closed	90	NA	Closed	Closed	1	6	Bridge	Simple
7	NA	Closed	90	NA	Closed	Closed	1	6	Bridge	Simple
8	NA	Closed	90	NA	Closed	Closed	1	5	Bridge	Bridge
9	NA	Closed	90	NA	Closed	Closed	1	7	Bridge	Simple
10	Closed	Closed	95	NA	Closed	Closed	1	8	Simple	Simple
11	Closed	Closed	100	NA	Closed	Closed	1	5	Bridge	Bridge
12	Closed	Closed	80	NA	Closed	Closed	1	5	Simple	Simple
13	NA	Unclosed	90	Unclosed	Closed	Closed	8	7	ND	Simple
14	NA	ND	ND	ND	Closed	Closed	6	7	ND	Simple
15	NA	ND	90	ND	ND	Closed	12	6	ND	Simple
16	NA	ND	100	ND	Closed	Closed	8	8	ND	Bridge

Bridge = bridge formation pattern; FD-OCT = Fourier-domain optical coherence tomography; Mh = macular hole; NA = not applicable (performed); ND = not done.

of 7 gas-filled eyes could be observed by TD-OCT on the day after surgery.[25] However, findings of the posterior retina depicted by TD-OCT would not necessarily prove MH closure because the macula is not identifiable in a gas-filled eye by several scans of TD-OCT. Especially in the immediate period after surgery, a foveal depression hardly exists in a gas-filled eye, which makes it more difficult to identify the macula correctly. In contrast, MH closure was confirmed reliably by FD-OCT, because it can cover a wider area by serially scanning every 40 μm. Indeed, 13 (81.3%) of 16 eyes could be examined clearly by FD-OCT during this period, which is much higher than that in Kasuga and associates' report (58%).[25] Without media opacity such as corneal haziness, it is likely that the more detailed postoperative morphologic features of the MHs can be examined by FD-OCT but not by conventional OCT immediately after surgery even in the eyes with gas tamponade. However, it is difficult to determine conclusively which is superior, because we did not perform a direct comparison using the same eyes in this study.

Using FD-OCT, the very early phase of the MH closure process after surgery was disclosed in detail. In the present series, a bridging formation of the neural retina was the first event after surgery. It seems that the neural retina was extended transversally, probably by the surface tension of the gas, release of tangential contraction by surgery, or both, resulting in so-called kissing or bridging of neural retina over the optically empty subretinal space. At day 1, these neural retinas were assumed to be just contacting each other, because gliosis or tissue repair was not likely to be completed within a day. However, as time advanced, the fistula-like structure became obscured and eventually disappeared. Possibly, as wound healing proceeded, the contacting retina fused with each other. At the same time, the subretinal space decreased over time (Figures 2 and 3). Interestingly, these processes are similar to those of spontaneous closure of the MH observed by OCT.[29,30] We believe that after the surface of the macula is sealed by tissue, it can keep contact using the negative pressure produced by fluid absorption in the RPE pump.[31] After this stage, no strong gas tamponade would be necessary and 1 day of face-down posturing may be sufficient.

Of important note is that the retinal cyst disappeared or was obscured before MH closure, which also was reported recently.[17] These findings support the hydration theory proposed by Tornambe.[31] We postulate that the critical factors for MH closure are relieving traction and isolating the hole from the vitreous fluid (posturing unnecessary), so that the intraretinal fluid can be pumped out by the RPE. This may be theoretical evidence that gas tamponade is not necessary for a long period.

Among 13 eyes that could be examined by FD-OCT within 2 days after surgery, 10 eyes showed signs of MH closure on day 1 (76.9%), 2 eyes on day 2 (15.4%), and 1 eye showed no sign of MH closure (7.7%). Although we did not have evidence, it is probable that 1 day of posturing would be sufficient for most eyes, but a prolonged tamponade would be necessary for some eyes to increase

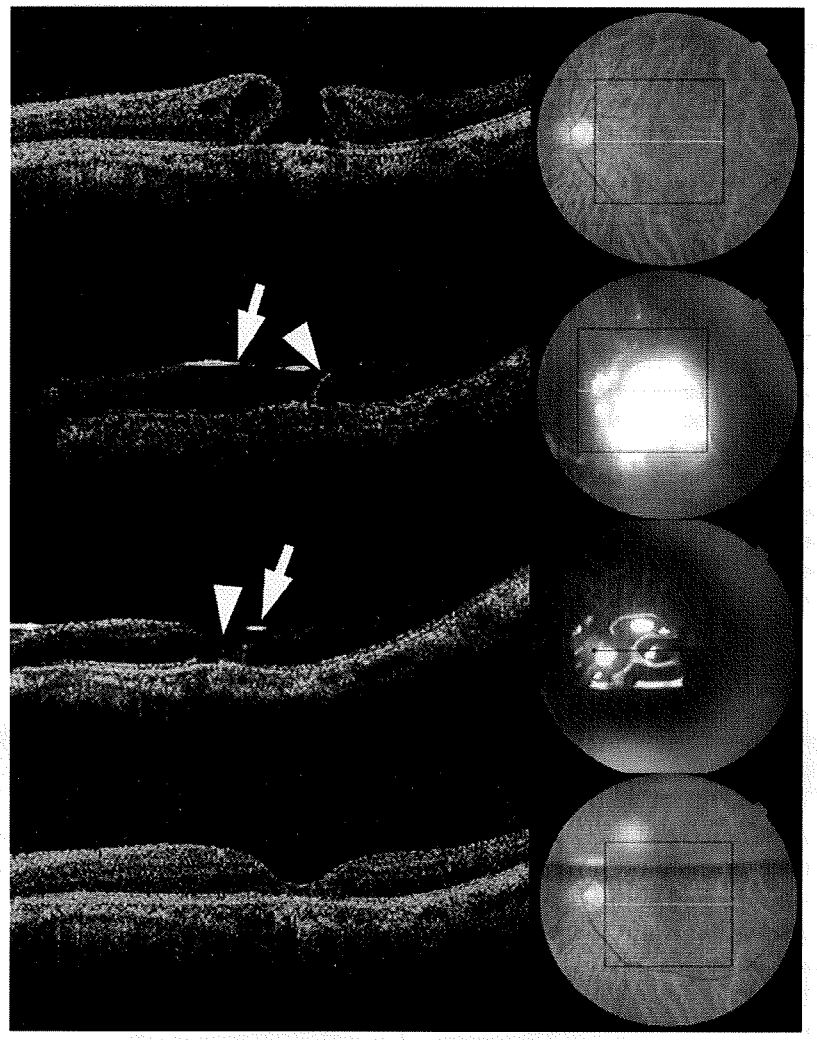

FIGURE 3. FD-OCT images and ocular fundus photographs after MH surgery obtained from Case 12 (eye 13). (Top row) Preoperative stage showing stage 3 MH. (Left) Several intraretinal cysts are found in the perifoveal retina. (Second row) One day after surgery. (Left) A fluid–gas interface is present (arrow). The neural retina at the temporal edge of the MH appears to be in contact with the retinal pigment epithelium, but there is a gap in the neural retina. The nasal edge of the MH is not well visualized in this image (arrowhead). (Right) A strong light reflex is noted in the ocular fundus. (Third row) Two days after surgery. (Left) Arrow indicates waterline. There is still a gap between the retina (arrowhead). (Right) A strong light reflex also comes from the posterior retinal surface. (Bottom row) 8 days after surgery. (Left) MH is closed with foveal depression. (Right) MH disappeared. An intraocular gas is still present. Square lines in the right figures show the area that was scanned serially by FD-OCT. Yellow or blue single lines also indicate the scanned sections shown on the left images.

the overall closure rate. To prove this, we would have had to stop posturing a patient with open MH and to demonstrate failure in such an eye, which would not be allowed ethically. Krohn reported that the success rate for 1 day of posturing was 87.5%, and for 1 week of posturing, it was 93.1%, although the results were statistically insignificant.[11] Hasler and Prünte performed surgery followed by 60% to 100% air tamponade with 2 days of posturing and observed that 90% of the MH was closed at day 2.[17] Their method of using a limited amount of air was superior because a rapid decrease of air allowed examination of the MH by OCT through the vitreous fluid from the early postoperative days. However, no additional tamponade is possible by continuing posturing, even if it is necessary. Hasler and Prünte performed the second surgeries for the eyes with unclosed MH in the early postoperative period. In contrast, in this study, 1 week of gas tamponade could close an MH that was found to be open at postoperative day 2 without any additional surgery (Case 12, eye 13). Phacovitrectomy with such a long-lasting gas as C_2F_6 is also a superior alternative method to avoid prolonged posturing,[16] but C_2F_6 gas remained for 4 to 6 weeks after surgery, and it would not be ideal for fast social rehabilitation.

There may be another concern with brief posturing. Takahashi and Kishi reported that a fragile or premature macula with a bridge formation was unstable and that

recurrence took place in such eyes.[19] Paques and associates reported that no evident cause of reopening was observed in most eyes with successfully closed MH and that reopening occurred after 8 months in that study; therefore, the length of posturing may not be an important factor for the recurrence of MH.[32] Although recurrence was not found in the present series, long-term follow-up is necessary.

Because all of the eyes in this study showed successful closure, the study provided no insight into whether posturing beyond 1 day was necessary for any patient. It is a theoretical possibility that we cannot answer from this study.

Our present method can be summarized as follows. Phacovitrectomy with ILM peeling is performed followed by full gas tamponade with 16% SF_6. Face-down posturing starts as immediately as possible after surgery. FD-OCT examination is performed from 3 hours to the day after surgery. When closure of the MH is confirmed, posturing is stopped. If not, posturing is continued until the macular area appears again below a gas-bubble (approximately 1 week). Using this method, most patients can be freed from needlessly prolonged posturing. A prolonged tamponade is carried out only for those who are found to have unclosed MHs within 2 days, which may not be saved by uniform short posturing.

We interpreted successful MH closure to have occurred after there was postoperative apposition of tissue across the fovea to bridge the MH. But, anatomic apposition may not necessarily equate with closure of MH. The bridge formation type of MH closure may represent incomplete closure where the central defect was too small to be imaged by FD-OCT rather than complete closure, because there is still SRF present. The simple closure pattern may well represent true MH closure, but could also just be apposition of the edges of the MH without a glial plug closing the hole. The intraocular gas-bubble remained in the eye, and it is likely that patients had some additional time when the gas-bubble contacted the MH because 16% SF_6 would last more than 1 week. Besides, other factors such as size and duration of the MH, duration of gas contact with the MH after surgery, or the use of ILM peeling may play a significant role. This should be remembered when interpreting the present results.

There are clear limitations in the present pilot study. Without question, the number of patients was small. The nonrandomized nature of patient selection carries a potential bias, and the sizes of MH were comparatively small. Some of these are inevitable with a prospective study. The present study was carried out during hospitalization, but there may be possible disadvantages for those with open holes or indeterminate imaging, because additional trips to the surgeon's office would be required as well as additional imaging studies in some cases. However, considering the noninvasiveness of the present method, the great merit of avoiding prolonged posturing, and the fact that no serious adverse event such as endophthalmitis was found, a tailor-made postoperative program based on early examination by FD-OCT after MH surgery should be justified. Although a further large-scale study is warranted, our present results emphasize the potential usefulness of FD-OCT in determining MH closure even at a very early postoperative stage with gas tamponade.

THIS STUDY WAS SUPPORTED IN PART BY A GRANT FROM THE RESEARCH COMMITTEE ON CHORIORETINAL DEGENERATION and Optic Atrophy, Ministry of Health, Labor, and Welfare, Japan, and by a Grant-in-Aid for Scientific Research from the Ministry of Education, Science, and Culture of the Japanese Government, Tokyo, Japan. The authors indicate no financial conflict of interest. Involved in design of study (K.Y., Y.S., N.D., T.S.); conduct of study (K.M., K.Y., Y.S., N.D., T.S.); management of data (K.M., K.Y., Y.S.); analysis of data (K.M., K.Y., Y.S., N.D.); interpretation of data (K.Y., Y.S., N.D., T.S.); overall coordination (T.S.); and preparation of the manuscript (K.M., K.Y., N.A., T.S.). This study was approved by the Kagoshima University Hospital Institutional Ethical Committee, Kagoshima, Japan (Institutional Review Board No. 16-3) and was performed in accordance with the Declaration of Helsinki. All patients gave informed consent before treatment.

REFERENCES

1. Kelly NE, Wendel RT. Vitreous surgery for idiopathic macular holes. Results of a pilot study. Arch Ophthalmol 1991;109:654–659.
2. Brooks HL Jr. Macular hole surgery with and without internal limiting membrane peeling. Ophthalmology 2000; 107:1939–1948.
3. Mester V, Kuhn F. Internal limiting membrane removal in the management of full-thickness macular holes. Am J Ophthalmol 2000;129:769–777.
4. Smiddy WE, Feuer W, Cordahi G. Internal limiting membrane peeling in macular hole surgery. Ophthalmology 2001; 108:1471–1476.
5. Benson WE, Cruickshanks KC, Fong DS, et al. Surgical management of macular holes: a report by the American Academy of Ophthalmology. Ophthalmology 2001;108:1328–1335.
6. Haritoglou C, Gass CA, Schaumberger M, et al. Long-term follow-up after macular hole surgery with internal limiting membrane peeling. Am J Ophthalmol 2002;134:661–666.
7. Verma D, Jalabi MW, Watts WG, Naylor G. Evaluation of posturing in macular hole surgery. Eye 2002;16:701–704.
8. Thompson JT, Smiddy WE, Glaser BM, et al. Intraocular tamponade duration and success of macular hole surgery. Retina 1996;16:373–382.
9. Tornambe PE, Poliner LS, Grote K. Macular hole surgery without face-down positioning. A pilot study. Retina 1997;17:179–185.
10. Isomae T, Sato Y, Shimada H. Shortening the duration of prone positioning after macular hole surgery: comparison between 1-week and 1-day prone positioning. Jpn J Ophthalmol 2002;46:84–88.
11. Krohn J. Duration of face-down positioning after macular hole surgery: a comparison between 1 week and 3 days. Acta Ophthalmol Scand 2005;83:289–292.

12. Sato Y, Isomae T. Macular hole surgery with internal limiting membrane removal, air tamponade, and 1-day prone positioning. Jpn J Ophthalmol 2003;47:503–506.
13. Tranos PG, Peter NM, Nath R, et al. Macular hole surgery without prone positioning. Eye 2007;21:802–806.
14. Ellis JD, Malik TY, Taubert MA, et al. Surgery for full-thickness macular holes with short-duration prone posturing: results of a pilot study. Eye 2000;14:307–312.
15. Simcock PR, Scalia S. Phacovitrectomy without prone posture for full thickness macular holes. Br J Ophthalmol 2001;85:1316–1319.
16. Dhawahir-Scala FE, Maino A, Saha K, et al. To posture or not to posture after macular hole surgery. Retina 2008;28:60–65.
17. Hasler PW, Prünte C. Early foveal recovery after macular hole surgery. Br J Ophthalmol 2008 ;92:645–649.
18. Madgula IM, Costen M. Functional outcome and patient preferences following combined phaco-vitrectomy for macular hole without prone posturing. Eye 2008;22:1050–1053.
19. Takahashi H, Kishi S. Tomographic features of early macular hole closure after vitreous surgery. Am J Ophthalmol 2000; 130:192–196.
20. Ho MD, Guyer DR, Fine SL. Macular hole. Surv Ophthalmol 1998;42:393–416.
21. Azzolini C, Patelli F, Brancato R. Correlation between optical coherence tomography data and biomicroscopic interpretation of idiopathic macular hole. Am J Ophthalmol 2001;132:348–355.
22. Hee MR, Puliafito CA, Wong C, et al. Optical coherence tomography of macular holes. Ophthalmology 1995;102:748–756.
23. Hangai M, Ojima Y, Gotoh N, et al. Three-dimensional imaging of macular holes with high-speed optical coherence tomography. Ophthalmology 2007;114:763–773.
24. Ko TH, Witkin AJ, Fujimoto JG, et al. Ultra-high resolution optical coherence tomography of surgically closed macular holes. Arch Ophthalmol 2006;124:827–836.
25. Kasuga Y, Arai J, Akimoto M, Yoshimura N. Optical coherence tomography to confirm early closure of macular holes. Am J Ophthalmol2000;130:675–676.
26. Ip MS, Baker BJ, Duker JS, et al. Anatomical outcomes of surgery for idiopathic macular hole as determined by optical coherence tomography. Arch Ophthalmol 2002; 120:29–35.
27. Sakamoto T, Miyazaki M, Hisatomi T, et al. Triamcinolone-assisted pars plana vitrectomy improves the surgical procedures and decreases the postoperative blood-ocular barrier breakdown. Graefes Arch Clin Exp Ophthalmol 2002;240: 423–429.
28. Sonoda KH, Sakamoto T, Enaida H, et al. Residual vitreous cortex after surgical posterior vitreous separation visualized by intravitreous triamcinolone acetonide. Ophthalmology 2004;111:226–230.
29. Yamada H, Sakai A, Yamada E, et al. Spontaneous closure of traumatic macular hole. Am J Ophthalmol 2002;134:340–347.
30. Milani P, Seidenari P, Carmassi L, Bottoni F. Spontaneous resolution of a full thickness idiopathic macular hole: fundus autofluorescence and OCT imaging. Graefes Arch Clin Exp Ophthalmol 2007;245:1229–1231.
31. Tornambe PE. Macular hole genesis: the hydration theory. Retina 2003;23:421–423.
32. Paques M, Massin P, Blain P, et al. Long-term incidence of reopening of macular holes. Ophthalmology 2000;107:760–765.

Biosketch

Kyoko Masuyama, MD, graduated in 2005 from Kagoshima University School of Medical and Dental Sciences, Kagoshima, Japan. Dr Masuyama currently does her ophthalmology residency at the Department of Ophthalmology, Kagoshima University.

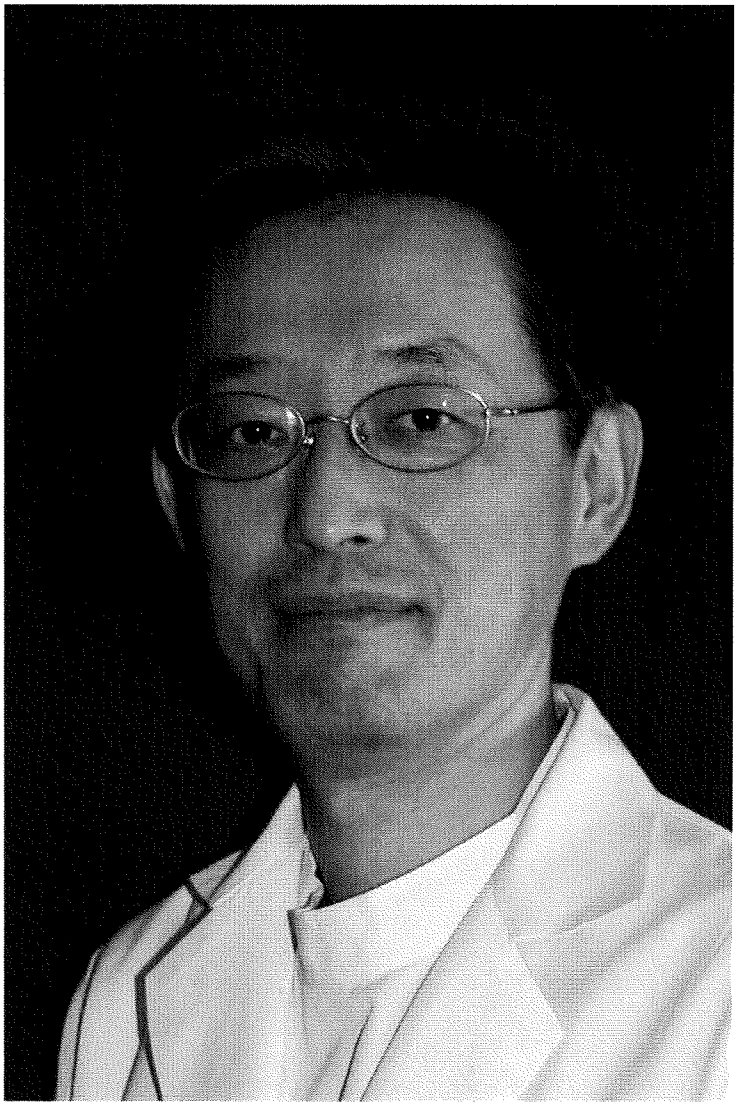

Biosketch

Taiji Sakamoto, MD, PhD, is the Professor and Chair, Department of Ophthalmology, Kagoshima University, Kagoshima, Japan. He completed residencies in Ophthalmology in 1985 and 1988 and fellowships in pathology at Kyushu University, Fukuoka, Japan. Dr Sakamoto was a lecturer of Doheny Eye Institute, University of Southern California, Los Angeles, California from 1992 to 1995. His research interests are ocular gene therapy, ocular neovascularization, and vitrectomy.